JOURNAL OF THEORETICAL AND APPLIED MECHANICS
42, 3, pp. 667-693, Warsaw 2004

APPLICATION OF NEUROCOMPUTING IN THE PARAMETRIC IDENTIFICATION USING DYNAMIC RESPONSES OF STRUCTURAL ELEMENTS – SELECTED PROBLEMS

Leonard Ziemiański
Bartosz Miller
Grzegorz Piątkowski

Department of Structural Mechanics, Rzeszów University of Technology
e-mail: ziele@prz.edu.pl

Some problems of neurocomputing in the dynamics of structures are presented: 1) damage detection using wave propagation, 2) updating of portal frames finite element models, 3) detection of the void and additional mass in cantilever plates, 4) neural network modelling of an "artificial boundary condition". The analysed problems are related to both data prepared by computational systems and that taken from experimental evidence.

Key words: neural networks dynamics, identification

1. Introduction

In recent years, interest in Artificial Neural Networks (ANN) has grown rapidly (Haykin, 1999; Waszczyszyn, 1999). The main reason is because of their powerful and adaptive abilities to treat various complex problems. Such a co-disciplinary approach can give solutions which are difficult to achieve by methods specializing in the analysis of inward-disciplinary oriented problems. Development of computer hardware and software causes, beyond doubt, formulation of new nonstandard methods of data processing. A wide range of applications were evoked by well known advantages of ANNs which offer complementary possibilities to computer sequential processing. This corresponds, first of all, to computer simulations of ANNs, sometimes called "neurocomputing".

In the paper, some results related to research done at the Faculty of Civil and Environmental Engineering of Rzeszów University of Technology are discussed in short. Only selected problems are reported, corresponding to dynamics of structures. In the paper, the main attention is given to Back-Propagation Neural Networks which are mostly used in the analysis of mechanical problems. The achieved results enable us to point out promising prospects of neurocomputing applications in dynamics of structures. Back-Propagation Neural Network (BPNN) applications in analysis of the following dynamics problems are discussed: (1) damage detection using wave propagation (Ziemiański and Piątkowski, 2000), (2) updating of portal frames finite element models (Miller and Ziemiański, 2001, 2003), (3) detection of the void and additional mass in cantilever plates (Piątkowski, 2003; Piątkowski and Ziemiański, 2003), (4) neural network modelling of an "artificial boundary condition" for infinite domains (Ziemiański, 2003). The analysed problems are related to both data prepared by computational systems and that taken from experimental evidence. Much attention was focused on preprocessing of input data and selection of the best type of a neural network and correct architecture. The influence of random noise inserted into data patterns on the neural network generalization process was analyzed. The results of performed calculations show that adding the noise to learning patterns significantly decreases values of MSE errors and increases resistance to the disturbance.

2. Damage detection using wave propagation

Non-destructive methods of detection of change of material properties and damage in structural elements present an important and valuable tool. These methods allow estimating the state of a structure as well as predicting a period of safety usage. An ultrasonic method is one of the most often used non-destructive methods (Thompson, 1983). For structures such as rods, plates, shells another widely used method is the one based on structural waves propagation. In this method, unlike in the classical method of ultrasonic testing, the wavelengths are large compared to the characteristic dimension of the structure, and a wave pulse propagates along the whole structure. Moreover, the excitation of structural waves is in one point while the measurements of structural waves velocity are in a few other points instead of surface scanning used in the ultrasonic testing. It simplifies the structural wave tests in rods, beams, plates and some other structures.

The Backpropagation ANNs with the Rprop learning algorithm were applied. Neural networks with one or two hidden layers were tested. The input vectors consisted of a preprocessed time signal. The outputs provided all parameters describing damage. Some of these parameters were identified by the network with satisfactory precision while other with a significant error. Based on the previous research done by the author (Ziemiański and Piątkowski, 2000). Cascade neural networks were built to improve the generalisation of networks. The first network was fed with the input vector as for a simple net. The first network's output is the most precisely determined parameter. The second network has got an input vector with an additional value of the parameter predicted by the first net. The output of this network is the next desirable parameter. The cascade networks with two or three stages were used (Figure 1).

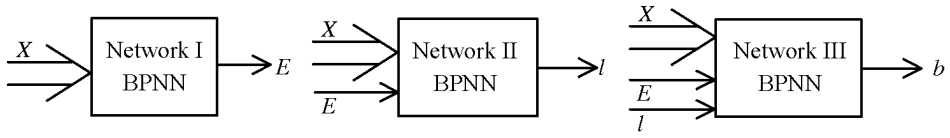

Fig. 1. A three stage cascade network

2.1. Preprocessing of signals

One of the used methods of preprocessing of input data was compression of a time signal (Ghaboussi and Lin, 1998; Haykin, 1999; Waszczyszyn and Ziemiański, 2004). The compression was performed by the dedicated neural network called replicator shown in Fig. 2.

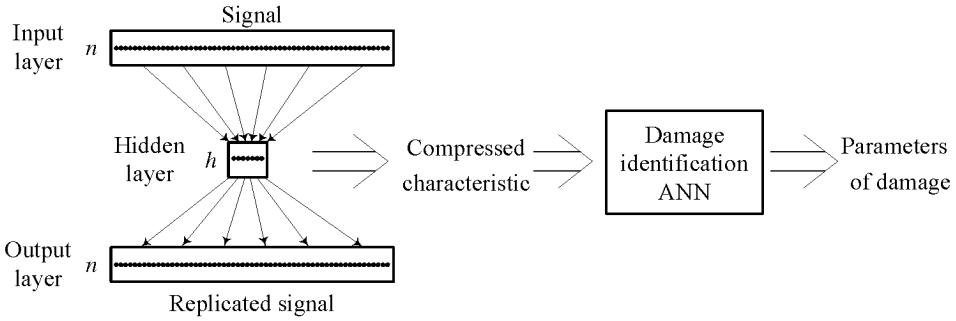

Fig. 2. The use of a replicator in a damage identification problem

Networks of architecture n-h-n were learned to replicate at the output the time signal data points given at the input – the input variables were mapped into the same output variables. The compression networks of 200-8-200 and 200-12-200 architectures were created. After training, the outputs from hidden neurons (see Fig. 2) were used as preprocessed data for the damage identification net.

2.2. Identification of cross-section changes

The next analysed task was a rod with a defect simulated as a notch (Ziemiański and Piątkowski, 2000). Removal of certain finite elements simulated the failure of the cross-section. Various widths $b = 0.1, \ldots, 1.1\,\mathrm{m}$, various heights $h = 0.1, \ldots, 0.8\,\mathrm{m}$ and various locations $l = 3.5, \ldots, 5.5\,\mathrm{m}$ of notch were considered (Figure 3a).

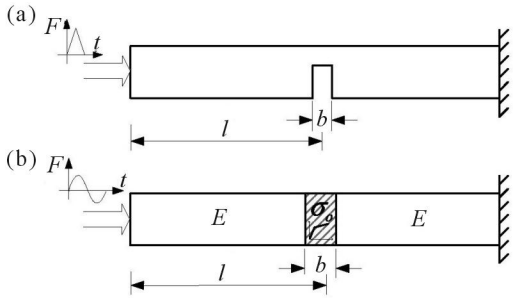

Fig. 3. A test on propagation of structural waves

Table 1. Comparison of errors of identification of cross-section parameters

St. par.	Height of defect		Location of defect		Width of defect	
	Learn	Test	Learn	Test	Learn	Test
	Standard net					
R^2	0.996	0.994	0.994	0.994	0.990	0.988
Stε	0.0149	0.0177	0.0193	0.0192	0.0215	0.0232
	Cascade net					
R^2	1.000	0.999	0.999	0.997	0.994	0.986
Stε	0.0043	0.0071	0.0094	0.0121	0.0165	0.0253

The input vector was described with values of first three peaks of the time signal (Ziemiański and Piątkowski, 2000) and by use of the replicator. Both standard and cascade nets were used at this stage. Better results were obtained from neural networks with two hidden layers. The width of the defect

has no influence on the quality of results. Damage identification is significantly better in the case of use of cascade networks. In Table 1 the results of neural simulation are put together.

2.3. Identification of the yielding zone

A group of finite elements with an elasto-plastic material occurred inside the rod. A plastic-bilinear material model was used. Young's modulus and strain hardening modulus were fixed. A failure was simulated by the change of yield stress σ_0. The width b and location l of the defect were changed (Fig. 3d). A concentrated force with a sine characteristic and duration of $400\,\mu$s was applied to the free end of the rod. The measured points were located behind the zone of yielding. For the identification networks the input vectors consisted of compressed time signals. A compression network with 8 neurons in the hidden layer was used. The output vectors consisted of three failure parameters (σ_0, b, l). When simple nets were used, the yield strength parameter and the location of the yield zone were identified correctly. The width of the defect was identified significantly worse. The use of cascade networks improved the identification of width of the defect (see Table 2).

Table 2. Learning errors in the identification of parameters of the yielding zone

St. par.	Yield stress	Location	Width
	Standard net		
R^2	0.922	0.995	0.769
Stε	0.0222	0.0117	0.0970
	Cascade net		
R^2	1.000	1.000	0.886
Stε	0.0039	0.0012	0.0680

3. Updating of finite element models of portal frames

3.1. Models and the experiment

This section presents an application of ANNs in updating models of two frames: one-storey portal frame and two-storey frame (Miller, 2002; Miller and Ziemiański, 2001). The height of both frames was 40 cm, the span was 46.9 cm.

The beam and columns had a rectangular cross-section of 2.6 cm by 0.6 cm. The beam-to-column connections and the footings were treated as rigid or flexible, depending on the used dynamic model.

Several FE models of each frame were built, the differences between them were as follows:

- the column footing and the beam-to-column connection were treated either as rigid or as flexible,
- the effective length of both columns was in the range of 40 cm (overall length of the columns) and 30 cm (the length of the columns above the steel connection plate); in dynamic models the columns length was 35 cm (flexible column footing) or 40 cm (clamped columns),
- the models were considered to be symmetrical or not.

Each model consisted of 12 (one-storey frame) or 16 (two-storey frame) finite beam elements and it had 39 or 48 DOFs. The laboratory models of both considered frames are shown in Fig. 4, while the FE models are shown in Fig. 5.

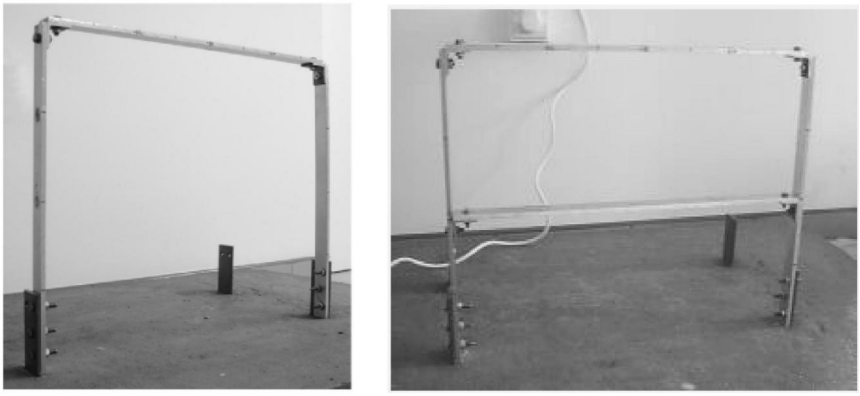

Fig. 4. Laboratory models of both considered frames

Vibrations of the laboratory models were excited by an impact. The response of the structure was measured in the range of 0 to 1024 Hz with the step of 0.25 Hz. The measurements were done using eight accelerometers attached in points corresponding to the nodes of the computational model. The FE models presented in this paper took into account concentrated masses corresponding to the masses of the accelerometers (10.2 g). The laboratory set-up involved PCB accelerometers, Brüel&Kjær modal hammer and CADA-X acquiring system with multichannel analyser Scadas III.

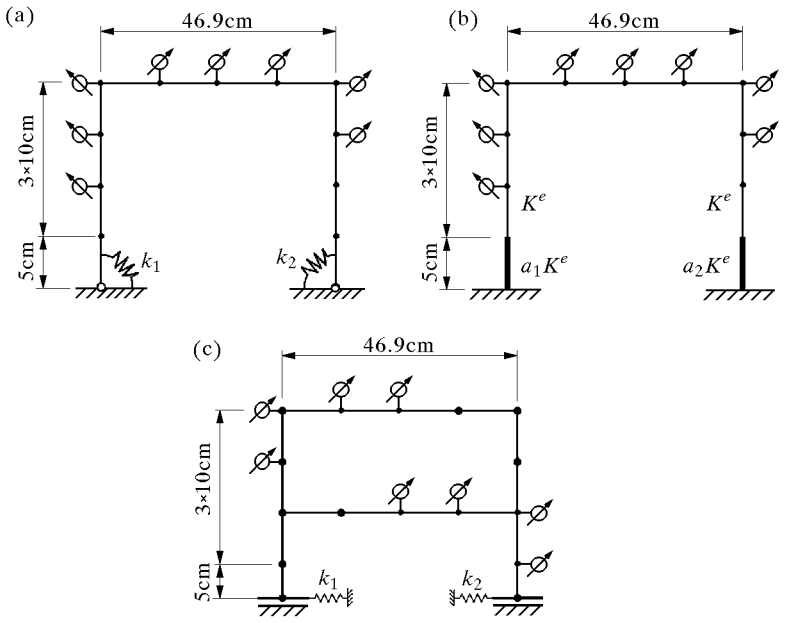

Fig. 5. The FE models of considered frames: (a) one-storey frame model FRAME1a, (b) one-storey frame model FRAME1b, (c) two-storey frame model FRAME2

3.2. The updating procedure

The model updating procedure consists of the following steps:

1. generation of a set of training data vectors based on the dynamic model,
2. training of the neural network with the training data,
3. exposition of expected data to obtain a set of changes,
4. application of the changes to the original model in order to generate a new model,
5. repetition of the previous steps if necessary.

This procedure leads to an updated model that can be updated again using the same method.

Multi layer feed-forward networks and networks with the radial basis function were used. The input information was the values of the first four eigenvalues. On the basis of eigenfrequencies, the networks updated one, two, three or four parameters of the models (for example rotational or translational stiffnesses of the supports and beam-to-column connection). The learning data were obtained from numerical simulations and then contaminated by an artificial

noise. The trained networks were fed on the data obtained from the experiment, and they predicted the updated values of selected model parameters. The updated models were then used to calculate the eigenfrequencies of the considered frames.

FRAME1a, FRAME1b and FRAME2 models were updated on the basis of measurements of the laboratory model with attached eight accelerometers.

3.3. Model FRAME1a

The updated parameters were the stiffnesses of the joints in column footings. The updating ANNs were of architecture 4-h-1, the learning and testing patterns were disturbed by the artificial noise (Gaussian) of variation 0.006. The number of learning patterns was equal to the number of the testing patterns, both sets consisted of 1005 patterns. The results of updating are shown in Table 3.

Table 3. The results of model FRAME1a updating on the basis of eigenfrequencies – symmetrical model

Eigenfrequency [Hz]	Measured value	Calculated value	Relative error
f_1	27.0	26	3.7%
f_2	81.5	85	−4.3%
f_3	169.8	174	−2.5%
f_4	176.5	182	−3.1%
RMSE $= 3.5 \times 10^{-2}$			

The RMSE is Root Mean Square Errors of the eigenfrequencies obtained from the updated model. RMSE is defined by the formula

$$\mathrm{RMSE} = \sqrt{\frac{1}{n-k+1}\sum_{i=k}^{n}\Big(\frac{f_{0i}-f_i}{f_{0i}}\Big)^2} \tag{3.1}$$

where

- k – first of considered eigenfrequencies
- n – last of considered eigenfrequencies
- i – number of eigenfrequency, $i = k, k+1, \ldots, n$
- f_{0i} – ith eigenfrequency obtained from "measurements"
- f_i – ith eigenfrequency obtained from numerical simulations.

The comparison of eigenforms obtained from numerical calculations and from measurements is shown in Fig. 6. The calculated eigenforms were, before the comparison, reduced using the static method (see Friswell and Mottershead, 1996).

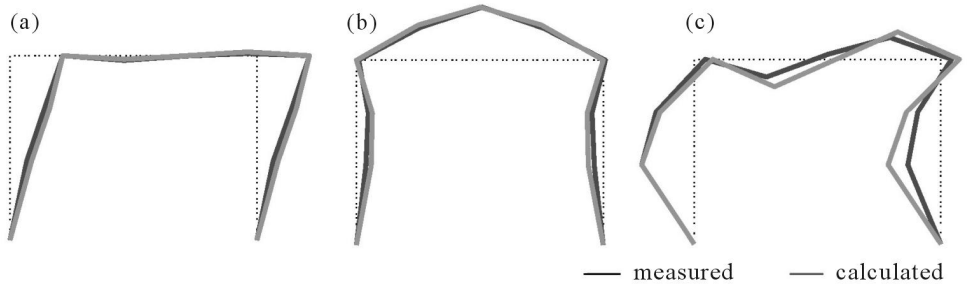

Fig. 6. The comparison of eigenforms obtained from calculations (symmetrical model FRAME1a) and from measurements: (a) first, (b) second, (c) third

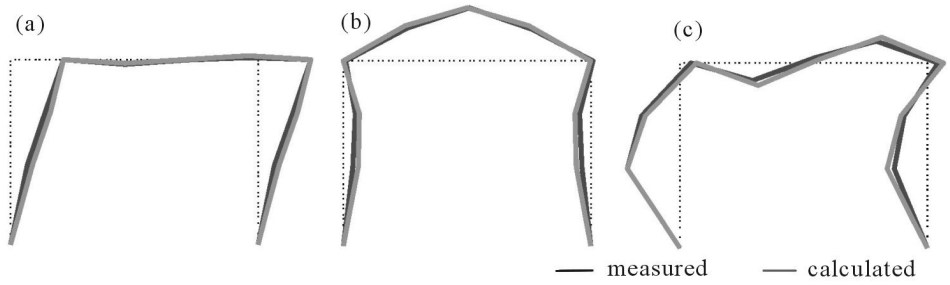

Fig. 7. The comparison of eigenforms obtained from calculations (non-symmetrical model FRAME1a) and from measurements: (a) first, (b) second, (c) third

The matrix MAC (see Friswell and Mottershead, 1996) for the first four eigenvectors is as follows

$$\mathrm{MAC}_{ij} = \begin{vmatrix} 0.9918 & 0.0008 & 0.2719 & 0.0288 \\ 0.0004 & 0.9845 & 0.0003 & 0.0044 \\ 0.1576 & 0.0000 & 0.9421 & 0.1060 \\ 0.0001 & 0.0084 & 0.0507 & 0.8873 \end{vmatrix}$$

The values on the main diagonal of the MAC matrix should be, in the case of proper updating, higher than 0.8, all other values should not exceed 0.1 (Friswell and Mottershead, 1996). In the presented matrix two elements have

values outside the expected range: $\mathrm{MAC}_{3,1}$ and $\mathrm{MAC}_{1,3}$ have values considerably higher than 0.1. It is caused by the linear dependence of adequate measured eigenforms. The MAC matrix calculated for measured eigenforms is as follows

$$\mathrm{MAC}_{ij} = \begin{vmatrix} 1.0000 & 0.0001 & 0.2099 & 0.0200 \\ 0.0001 & 1.0000 & 0.0000 & 0.0019 \\ 0.2099 & 0.0000 & 1.0000 & 0.0110 \\ 0.0200 & 0.0019 & 0.0110 & 1.0000 \end{vmatrix}$$

The elements $\mathrm{MAC}_{3,1}$ and $\mathrm{MAC}_{1,3}$ are twice as high as they should be.

The third and fourth eigenforms shown in Fig. 6c and Fig. 6d indicate that the considered frame in non-symmetrical. In the next step the values of the stiffnesses of the joints in the columns footings were updated independently. The ANNs were of architecture 4-h-2, the learning and testing patterns were disturbed by the artificial noise of variation 0.006. The number of learning and testing patterns was 5780 each. The results of updating are shown in Table 4, the comparison of eigenforms is shown in Fig. 7.

Table 4. The results of model FRAME1a updating on the basis of eigenfrequencies – non-symmetrical model435

Eigenfrequency [Hz]	Measured value	Calculated value	Relative error
f_1	27.0	26	3.7%
f_2	81.5	85	−4.3%
f_3	169.8	174	−2.5%
f_4	176.5	183	−3.7%
$\mathrm{RMSE} = 3.6 \times 10^{-2}$			

The matrix MAC for the first four eigenvectors is as follows

$$\mathrm{MAC}_{ij} = \begin{vmatrix} 0.9917 & 0.0010 & 0.2721 & 0.0275 \\ 0.0004 & 0.9847 & 0.0004 & 0.0041 \\ 0.1558 & 0.0001 & 0.9839 & 0.0390 \\ 0.0018 & 0.0081 & 0.0112 & 0.9499 \end{vmatrix}$$

The independent updating of rotational stiffnesses of both joints made it possible to obtain a model reproducing the eigenforms with a higher accuracy. The improvement is evident also in the MAC matrix, all elements on the main diagonal are equal or higher than 0.95.

3.4. Model FRAME1b

The frame with eight accelerometers was modelled also with clamped columns. The local stiffness matrices of the clamped elements were calculated as a product of the stiffness matrix of another column element (all others were the same) and the computational coefficient α, which was being updated. Model FRAME1b was updated with different values of coefficients α_1 and α_2, so the ANN was of architecture 4-h-2. The results of model FRAME1b updating are shown in Table 5.

Table 5. The results of model FRAME1b updating on the basis of eigenfrequencies

Eigenfrequency [Hz]	Measured value	Calculated value	Relative error
f_1	27.0	27	0.0%
f_2	81.5	85	-4.3%
f_3	169.6	169	0.5%
f_4	176.5	177	-0.3%
RMSE $= 2.2 \times 10^{-2}$			

The results are significantly better than those obtained from model FRAME1a. The error of eigenfrequency prediction exceeds 4% only for the second eigenfrequency f_2, in other cases the error is smaller than 1%. The matrix MAC for the first four eigenvectors is as follows

$$\mathrm{MAC}_{ij} = \begin{vmatrix} 0.9918 & 0.0008 & 0.2719 & 0.0288 \\ 0.0004 & 0.9845 & 0.0003 & 0.0044 \\ 0.1576 & 0.0000 & 0.9421 & 0.1060 \\ 0.0001 & 0.0084 & 0.0507 & 0.8873 \end{vmatrix}$$

3.5. Model FRAME2

The comparison of exemplary results obtained from the updated model (Fig. 5c) and the data measured on the laboratory model are shown in Table 6.

The accuracy of the updated model was determined by the comparison of the eigenforms and eigenfrequencies obtained from the measurements and from the updated model, the maximum difference between the measured and calculated eigenfrequencies did not exceed 5%, which must be considered as a very good result. The results obtained from the updated models are precise in the range of the eigenfrequencies used as input information of the ANNs.

Table 6. The results of updating of the FE model of the two-storey frame

Eigenfrequency [Hz]	Measured value	Calculated value	Relative error
f_1	33.0	312	3.0%
f_2	91.1	95	−4.3%
f_3	106.1	105	2.9%
f_4	123.0	121	1.6%
RMSE $= 3.1 \times 10^{-2}$			

4. Detection of the void and additional mass in a cantilever plate

The assessment of the structure state is a task which requires continuous researches and their development. There are a lot of methods based on a non-destructive testing of structural elements. Some of these methods utilize dynamical parameters of the monitored structure, such as modal characteristics (resonance frequencies), response of the structure to an impulse forcing and structural waves analysis (Yagawa and Okuda, 1996). One of the most important objectives of these methods are detection and localisation of changes, failures and defects in structural elements. This section presents the possibility of application of Artificial Neural Networks (ANN) for non-destructive detection of a circular void and additional mass in cantilever plates. Detection methods are based on the analysis of eigenfrequencies and analysis of the structure response to a harmonic excitation. The backpropagation neural networks with the Levenberg-Marquardt training function were applied. Standard networks and cascade sets of MLFF backpropagation neural networks were used (Waszczyszyn and Ziemiański, 2001; Piątkowski and Ziemiański, 2002).

4.1. Identification of a circular hole location

Numerical tests were carried out for rectangular plates with an internal defect in the form of a circular hole (Piątkowski and Ziemiański, 2003). The geometry of a plate is presented in Fig. 8. The plate has a unit thickness. The position of the void centre is defined by two parameters which are OY and OZ coordinates. These coordinates and the diameter are unknown parameters of the inverse problem.

The extreme locations of centre of the hole are located 0.05 m from the plate edges. The location of the void is changed with a step of 0.01 m. It has

given 341 different positions. In eigenproblem analysis, due to symmetry of the plate, only the 186 different positions of the hole are taken under consideration. The centres are located under or on the axis of symmetry of the plate.

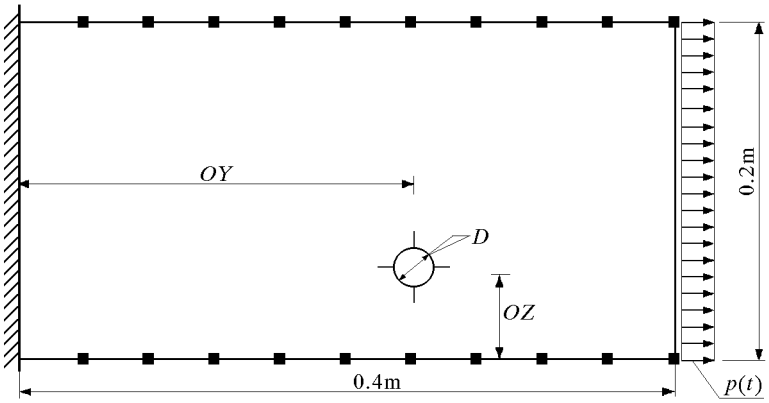

Fig. 8. The numerical model of the plate-scheme and main dimensions

For each considered location of the void, a FEM model of the plate was found by means of the Adina finite element system. Numerical models were made of 2D solid plane stress elements [1]. Thus, only the in-plane vibrations of the plate were analysed. The meshes of elements were generated automatically on the basis of sets of solid geometry faces.

An isotropic linear elastic material model was used. The plate had the following material properties: Young's modulus $E = 215\,\mathrm{GPa}$, Poisson's ratio $\nu = 0.3$, density $\rho = 7850\,\mathrm{kg/m^3}$.

The artificial neural network analysis of the calculated eigenfrequencies was performed to find the hole centre coordinates and its diameter.

The first neural experiment consisted in identification of two coordinates of the centre of the void with diameter $D = 0.002\,\mathrm{m}$ on the basis of eigenfrequencies. The computations showed that the acceptable accuracy could be achieved by the input vector, which composed of only five elements. These elements included relative changes of first five eigenfrequencies. The relative changes were calculated as follows

$$\Delta f_i = \frac{f_i - f_i^o}{f_i^o} \tag{4.1}$$

where f_i^o are the eigenfrequencies of the homogeneous plate (without a void) and f_i respective values corresponding to the plate with the void.

Better results were obtained from a cascade network (Piątkowski and Ziemiański, 2002). The maximum error of prediction of centres locations for the training data set was 1.4 mm and for the testing dataset was 1.5 mm. The identified locations are shown in Fig. 9, where the centers from the training and testing sets are marked by $\boldsymbol{x}$ in gray and black colours. This figure shows the lower half of the plate due to symmetry of the solution to the eigenproblem for the plate under consideration.

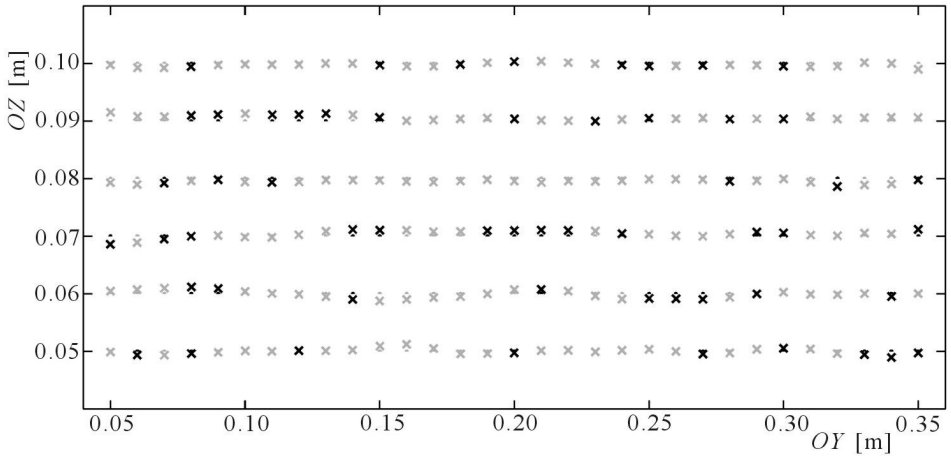

Fig. 9. Results for the $OY \triangleright OZ$ cascade network of architecture $5-7-1 \triangleright 6-7-1$

Next, the identification of three parameters of the void $\{OY, OZ, D\}$ was performed. In this task, the number of void positions was decreased to 39. The voids were located in the lower half of the plate. Nine diameters of each void were simulated in the range of 0.004-0.02 m. Thus, the total number of patterns was 351. Relied on experiences from the previous expirement, a three-stage cascade neural network was applied. It was experimentally determined that the best results were obtained by the cascade network with the following prediction order of parameters: $D \triangleright OY \triangleright OZ$.

The results presented in Fig. 10 multiple marks $\boldsymbol{x}$ which relate to different diameters of voids at a given position. One can see that the vertical coordinate of voids was predicted with a higher error than the horizontal one.

The histograms presented in Fig. 11 show that the maximum relative error of the OY coordinate identification was $\pm 2\%$, both for the training and testing sets of patterns. The OZ coordinates were predicted with a relative error of $\pm 10\%$. The third parameter of the void, its diameter, was identified with a relative error of $\pm 4\%$ in the diameter range 0.004-0.020 m.

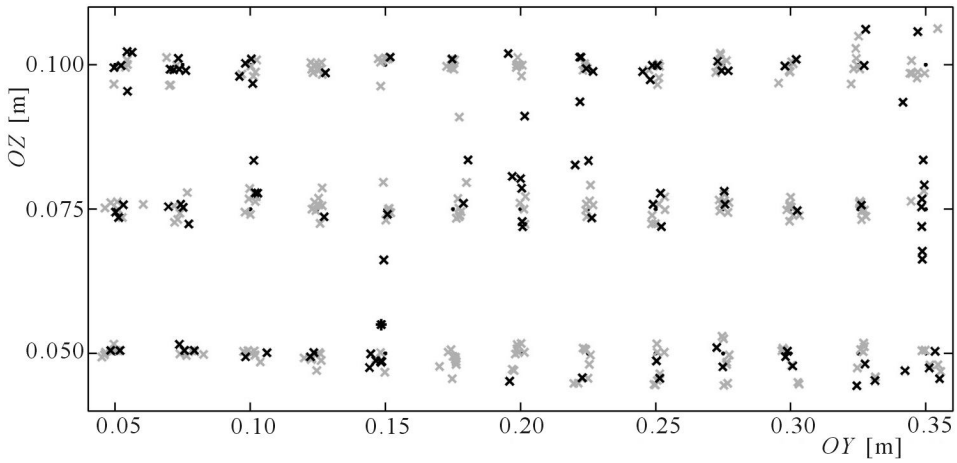

Fig. 10. Results for the $D \triangleright OY \triangleright OZ$ cascade network of architecture 5-7-1▷6-7-1▷7-7-1

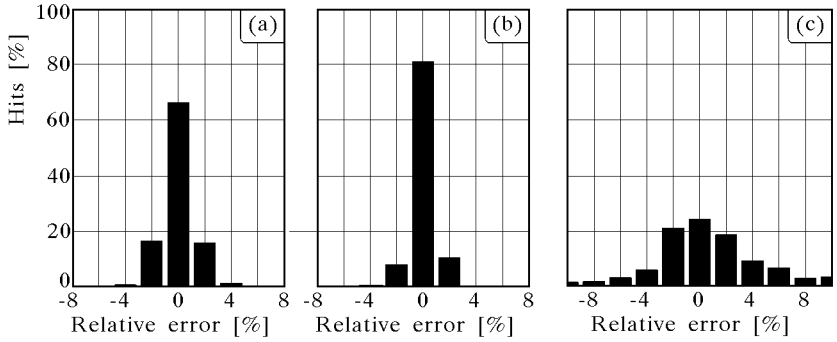

Fig. 11. Histograms for (a) diameter of the hole D, (b) coordinate OY, (c) coordinate OZ for $D \triangleright OY \triangleright OZ$ cascade network of architecture 5-7-1▷6-7-1▷7-7-1

4.2. Detection of an additional mass

Two laboratory models were built as it is shown in Fig. 12 (Waszczyszyn and Ziemiański, 2004). The models were made of steel and aluminium alloy plates, fixed to a massive stand by high-tensile bolts.

The experimental set consisted of eight PCB acceleration sensors. Scadas III analyzer with LMS software was applied to measure the response of the structure. The out-plane vibrations of the plate were forced with a modal hammer. The locations of sensors and the point of impact are shown in Fig. 12b.

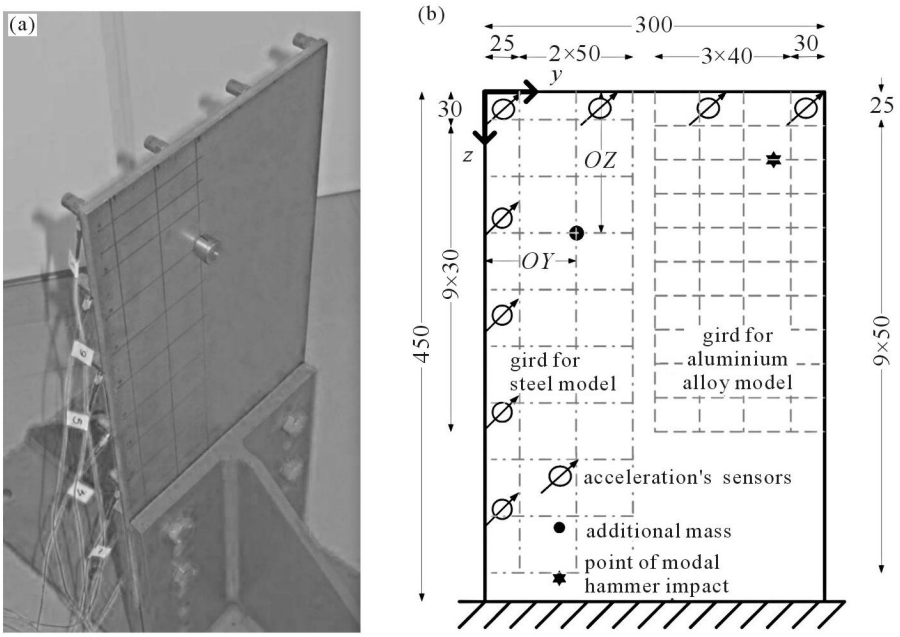

Fig. 12. (a) The experimental model of the steel plate, (b) scheme of the plate, main dimensions

The additional mass, whose position was detected, had a mass of 3% or 8% of the plate mass, respectively for the steel or the aluminium alloy models. The mass was located in nodes of the measurement grid. The grids for both models are shown in Fig. 12b. The 27 locations of the additional mass in the steel model were considered. For the aluminium alloy model the grid was changed. Thus, the vibrations of the plate for 40 locations of the additional mass were measured.

The acceleration signals in the time domain were transformed by means of Fast Fourier Transformation into the frequency domain. The obtained frequency characteristics had resolution of 0.25 Hz. These characteristics were analysed in selected bands. Consequently, within these bands the harmonics with the highest amplitudes were searched out. Finally, the sets of frequencies of vibration of the plates with the additional mass were obtained.

The total number of frequency characteristics was equal to $8 \cdot 27 = 216$ as the result of conducting of measurements with eight sensors for 27 locations of the mass. The set of frequencies for the steel plate consisted of $[216 \times 5]$ frequencies, because a searc for modal frequencies within five selected bands was performed. The inputs vectors for ANN training were prepared by a process

of elimination of outstanding measurements. After that, the average frequency in each band for each location of the mass was calculated. Consequently, the $[27 \times 5]$ input data set was prepared for the training of the networks used for mass identification.

In the case of the aluminium alloy plate the number of frequency characteristics was much higher and was equal to 1528. The number of 1528 characteristics was a result of considering 40 locations of the mass, conducting measurements with eight sensors and recording plate vibrations for at least three hammer impacts. These characteristics were analysed in six selected bands. Finally the $[1528 \times 6]$ set of characteristics was obtained. In order to prepare input data, on averaging of the whole set of frequencies was performed using neural networks. Six networks of 2-10-1 architecture were built – separately for six bands. These networks were learnt to re-map the two coordinates of the additional mass into modal frequency within the selected band. Consequently, the $[40 \times 6]$ input data set was prepared.

Due to a small number of patterns (27 for the steel plate and 40 for the aluminium alloy plate) it was decided to find additional patterns by adding the artificial Gaussian noise with the variance $\sigma = 0.001$. The number of patterns was increased to four hundreds that way. The two coordinates of location of the additional mass were determined separately by means of neural networks of architecture 5-5-1. 10% of the patterns was selected to testing.

Table 7. Statistical parameters for networks 5-5-1 and 5-5-2

	5-5-1		5-5-2	
	OY	OZ	OY	OZ
R^2	0.992	0.991	0.939	0.980
$\mathrm{St}\varepsilon \cdot 10^2$	2.97	2.60	8.21	3.75

Next, two coordinates of location of the additional mass were determined by means of the neural network of architecture 5-5-2. Statistical parameters, which describe the trained networks are collected in Table 7. The first part of this table refers to two 5-5-1 networks, which were used for separate determination of two coordinates of location of the additional mass. The second part refers to 5-5-2 network. This network did not manage to determine both coordinates simultaneously.

The results of the identification of location of the mass are presented in Fig. 13a. The horizontal and vertical bars are proportional to standard deviation of determination of the OY and OZ coordinates due to noised input vectors. The best accuracy was obtained from the $OY \triangleright OZ$ cascade neural

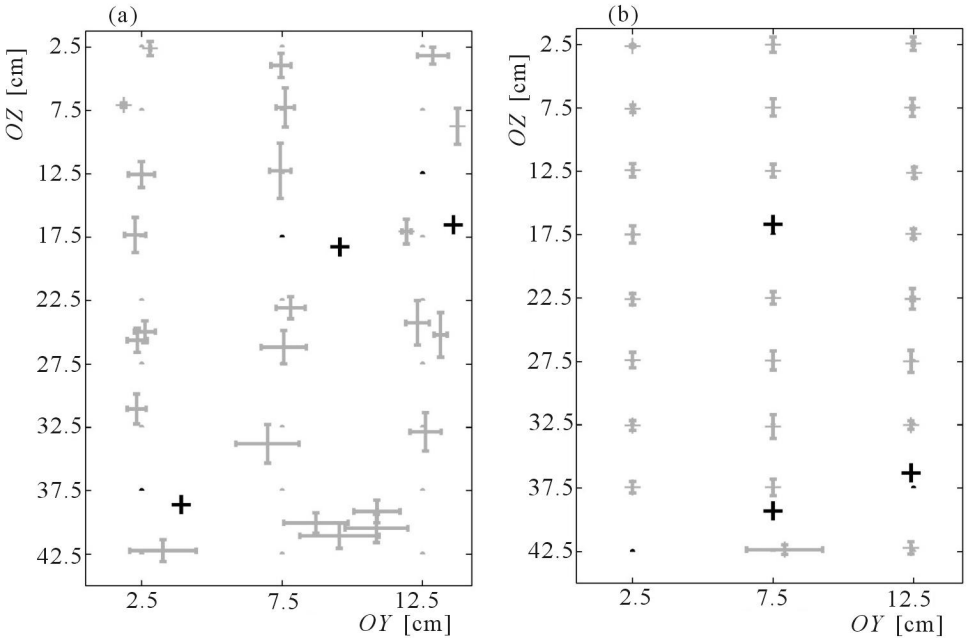

Fig. 13. Results of the identification of the additional mass in the steel plate, (a) standard network 5-5-2, (b) cascade network 5-5-1▷6-5-1

network of architecture 5-5-1▷6-5-1. The results for the training (gray marks) and testing sets (black marks) are shown in Fig. 13b.

For the aluminium alloy plate, the results were analogous to those obtained for the steel model. Again, the best determination of location of the additional mass was obtained from the cascade network, which was fed with the input vector noised with the variance $\sigma = 0.001$.

The results for the training (gray marks) and testing patterns (black marks) are shown in Fig. 14.

5. Modelling of an "artificial boundary condition" by neural network

In many fields of engineering an infinite or semi-infinite domain (unbounded structure) has to be analyzed. This kind of structure is considered in wave propagation problems such as soil-structure interaction, fluid-structure interaction, acoustics, electromagnetism and so on Wolf and Song (1996), Givoli

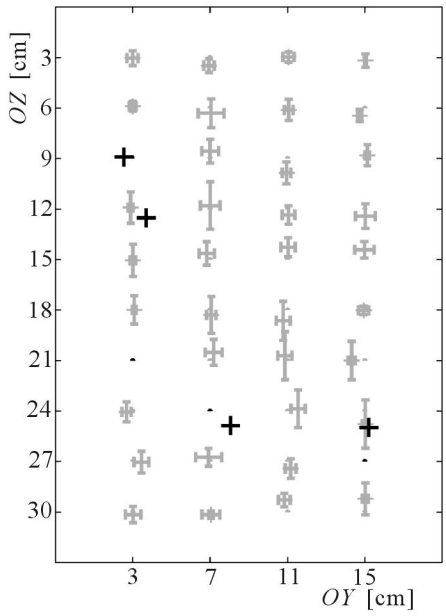

Fig. 14. Results of the identification of the additional mass in the aluminium alloy plate – cascade network 6-5-1▷7-5-1

(1992). The numerical study of problems originally formulated on unbounded domains requires the implementation of special techniques for the treatment of "infinity". A number of methods were formulated for the reduction of the problem to a bounded domain such as direct and indirect boundary element methods, infinite elements, DtN method (Wolf and Song, 1996; Givoli, 1992). One of the corresponding techniques is based on an artificial truncation of the original infinite domain at a certain distance away from the region of interest, which implies that one must set special boundary conditions on the external (artificial) boundary of the newly formed finite computational domain. A surface which encloses the most important part of the structure is often introduced. The model can be obtained by the application of an approximate boundary condition to the artificial surface – the so called Artificial Boundary Condition (ABC). In wave propagation problems, ABC is also the called non-reflecting boundary condition or transmitting boundary (Givoli, 1992).

The modelling of the transmitting boundary using neural networks was discussed by Ziemiański (2003). The assumption that the simulation of the artificial boundary condition on the artificial surface is carried out by corresponding neural networks is made (Ziemiański, 2003). The task of these neural

networks is to simulate boundary conditions fulfilling the radiation condition and avoiding appearance of the reflected wave. Back Propagation Neural Networks are used for this task (Waszczyszyn and Ziemiański, 2001).

5.1. A semi-infinite strip with notch

In the presented example the wave propagation in a semi-infinite strip with notch is discussed (see Fig. 15).

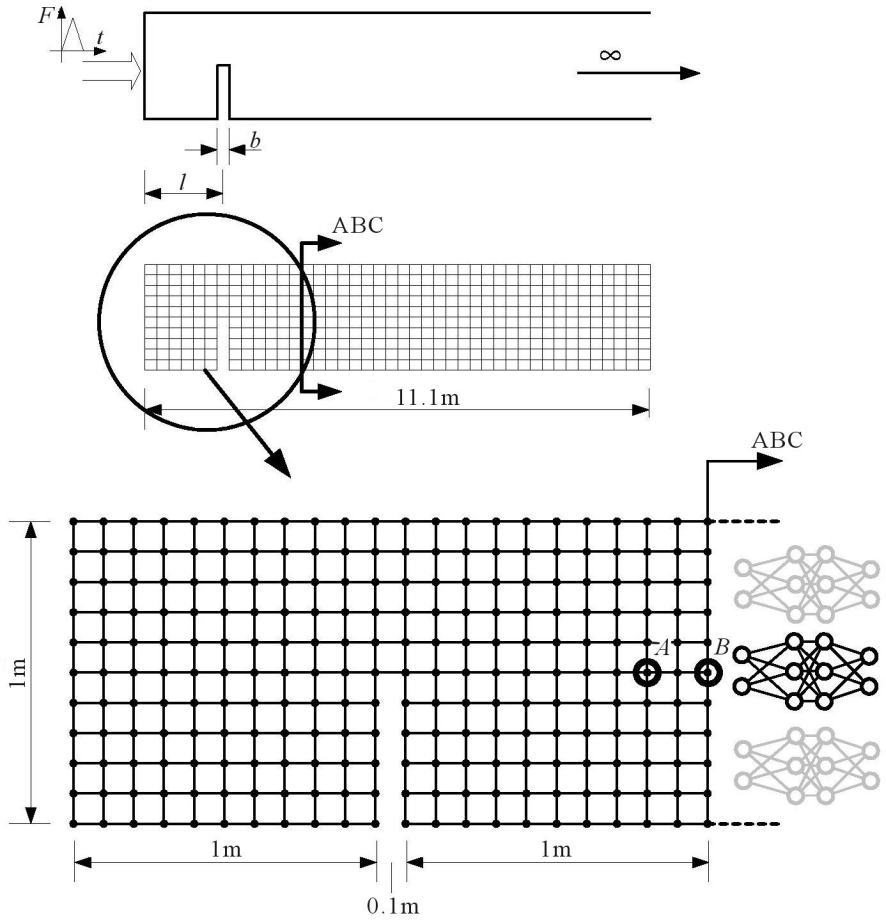

Fig. 15. A semi-infinite strip: (a) analyzed problem, (b) finite element mesh for the extended model, (c) finite element mesh for the truncated model

The wave originates at the free end of the rod by a displacement excitation in the form of a pulse with various durations and amplitudes. An extended finite element mesh (Fig. 15b) was used for computation of dynamic responses

in the nodes placed on the artificial boundary. The results of computation were used to train the back-propagation neural network (BPNN). The input for the neural network was defined as a vector including horizontal and vertical displacements at the time $t-1$ in three consecutive nodes on the line perpendicular to the artificial boundary. The output vector determines the dynamic reactions $\boldsymbol{R}(t)$ (two components R_h and R_v) in nodes on the truncated boundary (ABC) at the time t.

The learning patterns were obtained from the extended FE mesh. The trained neural network predicted the dynamic reactions $\boldsymbol{R}(t)$, which were checked by the comparison of the displacement, velocities and accelerations of selected nodes obtained from the extended mesh and those obtained from the truncated model with the neural networks used for the prediction of the dynamic reactions on ABC. After some calculations and multi-fold cross-validations, two-hidden-layer networks of architecture 6-12-8-2 were applied and the responses of the truncated hybrid NN/FE model were computed. In the Fig. 16 the response of horizontal and vertical displacements are displayed and traces of the difference between two signals are also shown.

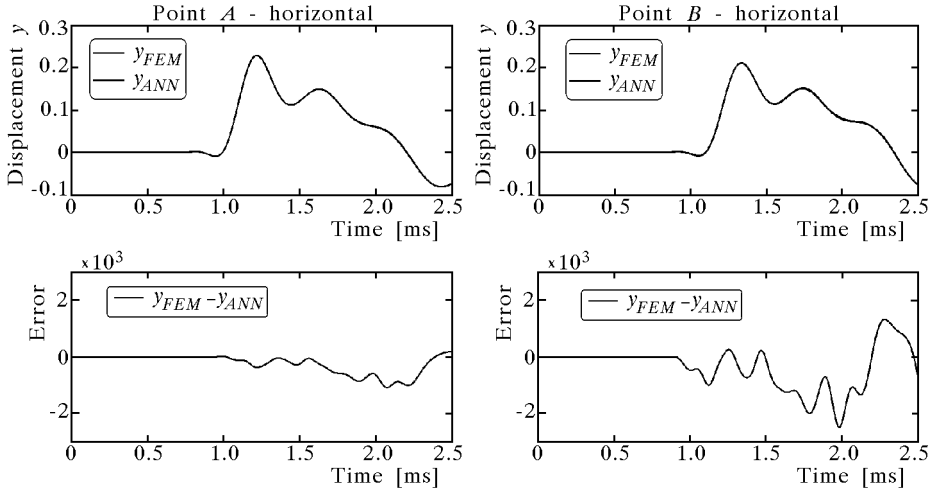

Fig. 16. Responses of horizontal displacements at points A and B and errors of displacements

5.2. A semi-infinite wedge

In the second example, the wave propagates in a semi-infinite wedge fixed on one edge, along the direction of the wave propagation. The considered FE

model is shown in Fig. 17. The wedge angle equals 30 degrees, the distance from the center of the angle to the beginning of the wedge and the width of the wedge both equal 80 m. The wave originates at the narrower (internal) end of the wedge by the horizontal displacement excitation with various durations t and amplitudes A (see Fig. 18a). The excitation is triangle-shaped, with the amplitude A varying with the location on the excitated edge from zero at the bounded end of the edge to the maximum value at the free end of the edge.

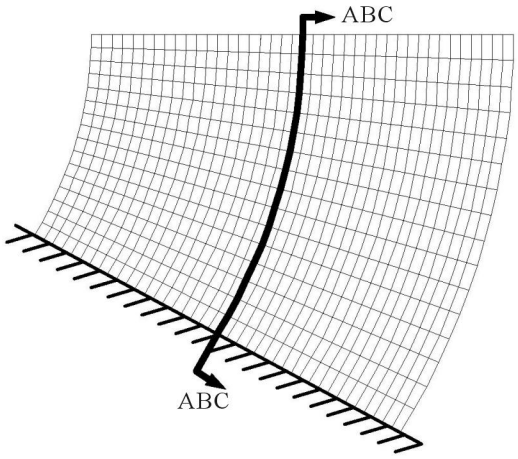

Fig. 17. A semi-infinite wedge: FE mesh

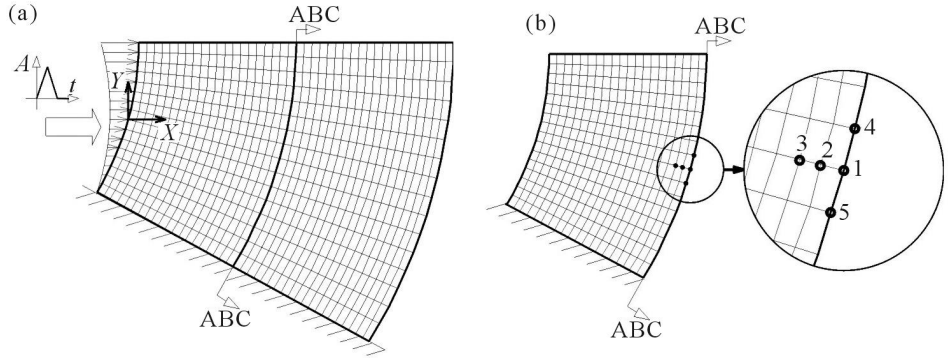

Fig. 18. (a) The triangle-shaped displacement excitation; (b) selected nodes of FE mesh

The extended model, shown in Fig. 15d, is used for computation of dynamic responses in the nodes located at the artificial boundary. The values of displacements, velocities and accelerations at the time $t-1$ calculated at selected points using the extended model were used to build up the input vector of neural networks. The output vector determined the dynamic reactions $\boldsymbol{R}(t)$ in nodes on the ABC at the time t. The learned network was used to predict the reactions, which were applied to the truncated model in order to avoid the reflection of the propagating wave.

The BPNN networks trained using the Levenberg-Marquardt algorithm were applied. The networks had one or two hidden layers, the output vector consisted of the values of two components (horizontal and vertical) of the dynamic reaction in a selected point. The input vector consisted of:

- horizontal and vertical components of displacements of three consecutive points on the line perpendicular to the artificial boundary (points 1, 2 and 3 in Fig. 18b)
- horizontal and vertical components of displacements of three consecutive points on the line perpendicular to the artificial boundary and the dynamic reaction in point 1 (see Fig. 18b) at the time $t-1$
- horizontal and vertical components of displacements of four points (points 1, 2, 4 and 5 in Fig.18b)
- horizontal and vertical components of the displacement, velocity and acceleration in point 1.

The dynamic reaction was predicted only in point 1, in the middle of the artificial boundary. The accuracy of the neural prediction was determined by the comparison of the data obtained from the extended FE model and from the truncated model with dynamic reactions applied to the artificial boundary (one of them was predicted by the neural network).

In order to train and test the neural network 61 different excitation signals were generated. The dynamic reaction in each point on ABC was calculated numerically in 326 time moments with the step $\Delta t = 20 \times 10^{-6}$ s. The overall time of observation was 0.0065 s. The excitation signals had different durations and amplitudes. The duration of the excitation signal varied from 1.2×10^{-4} s to 3.6×10^{-4} s with the step of 0.48×10^{-4} s (6 different values). The amplitude of the signal varied from 6×10^{-2} to 14×10^{-2} with the step of 1.6×10^{-2} (6 different values), so together 36 excitation signals and 36 sets of dynamic reactions (each consisting of 326 points) were obtained. The second set of excitation signals and dynamic reactions, used to test the neural network, was

obtained using 5 different durations and 5 different amplitudes (with values between the values used to generate the learning signals). The number of testing signals and the number of sets of dynamic reactions equaled 25.

In the first of considered examples, the input vector consists of six values: vertical and horizontal displacements in points 1, 2 and 3 at the time $t-1$. The neural network was trained to predict the vertical and horizontal dynamic reaction in point 1 at the time t. The learning set consisted of 11700 patterns (36 excitation signals, 326 dynamic reactions calculated using each excitation signal, one reaction rejected from each group in order to obtain patters consisting of inputs at the time $t-1$ and outputs at the time t). The testing set consisted of 8125 patters (25 excitation signals, 326 minus 1 dynamic reactions). Two hidden layer networks of architecture 6-12-8-2 were applied. The network was able to predict the dynamic reaction on the basis of the displacements in the input vector. However, the goal of the ANN application was not to predict the proper values of dynamic reactions but to obtain the truncated model with the transmitting boundary, without the excitation due to the reflected wave. The results of calculations done using the truncated model were used to test the accuracy of the artificial boundary built using the neural networks.The results obtained from this network are presented graphically in Fig. 19.

6. Final remarks

On the basis of the achieved results, the following conclusions can be drawn:

- ANNs can be efficiently applied in the field of dynamics of structures
- ANNs can deal with data prepared by computational systems and those taken from experiments (also the data can be mixed)
- ANNs make it possible to use structural wave propagation analysis for detection and assessment of damage in structural elements
- the hybrid approach (neural network – finite element) proves to be an effective tool to solve the problem of the model updating
- ANNs can be effectively used as a tool for non-destructive detection of a void and additional mass in plates

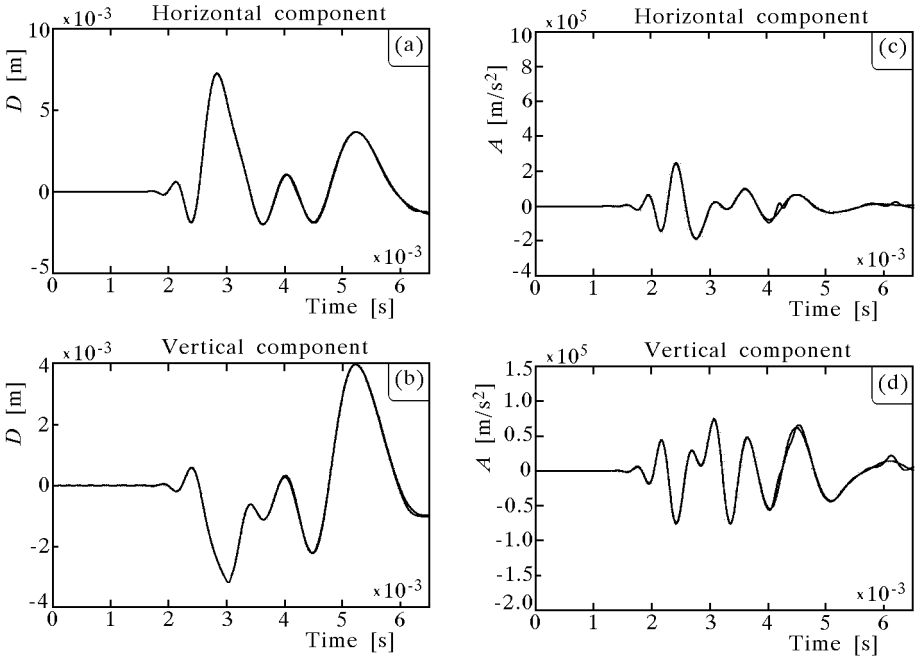

Fig. 19. Displacements (a,b) and accelerations (c,d) in point 1 in relation with the time calculated using the truncated model and 8-12-8-2 network in *closed loop* (the input vector consists of displacements in points 1, 2 and 3)

- BPNNs can be efficiently applied to the implementation of an approximate boundary condition on an artificial surface.
- Application of cascade networks improves accuracy of neural approximation in all analysed cases.

References

1. ADINA System Online Manuals, Theory and modeling guide, 2001, ADINA R&D Inc., Watertown
2. Friswell M.I., Mottershead J.E., 1996, *Finite Element Model Updating in Structural Dynamics*, Kluwer Academic Publishers, Dordrecht
3. Ghaboussi J., Lin C-C.J., 1998, New method generating spectrum compatible accelerograms using neural networks, *Earthquake Engineering and Structural Dynamics*, **27**, 377-396

4. GIVOLI D., 1992, *Numerical Methods for Problems in Infinite Domains*, Elsevier, Amsterdam

5. HAYKIN S., 1999, *Neural Networks, a Comprehensive Foundation*, second ed., Prentice Hall, Upper Saddle River

6. MILLER B., 2002, Updating of Mathematical Models of Engineering Structures (in polish), PhD dissertation, Rzeszów University of Technology

7. MILLER B., ZIEMIAŃSKI L., 2001, Updating of mathematical models using neural networks, *Proc. 2nd European Conference on Computational Mechanics*, Kraków, **I**, 386-387

8. MILLER B., ZIEMIAŃSKI L., 2003, Neural Networks in Updating of Dynamic Models with Experimental Verification, In: L. Rutkowski, J. Kacprzyk, eds., *Advances in Soft Computing*, Physica-Verlag a Springer-Verlag Company

9. PIĄTKOWSKI G., 2003, Detection of Damage in Structural Elements Using Artificial Neural Network (in polish), PhD dissertation, Rzeszów University of Technology

10. PIĄTKOWSKI G., ZIEMIAŃSKI L., 2002, Identification of Circular Hole in Rectangular Plate Using Neural Networks, *Proceedings of AI-Meth Symposium on Methods of Artificial Intelligence*, 329-332

11. PIĄTKOWSKI G., ZIEMIAŃSKI L., 2003, Neural network identification of a circular hole in the rectangular plate, In: L. Rutkowski, J. Kacprzyk, eds., *Advances in Soft Computing*, Physica-Verlag a Springer-Verlag Company

12. THOMPSON R.B., 1983, Quantitative ultrasonic nondestructive evaluation methods, *Journal of Applied Mechanics*, 1191-1201

13. WASZCZYSZYN Z., EDIT., 1999, *Neural Networks in the Analysis and Design of Structures*, CISM Courses and Lectures No. 404, Springer, Wien-New York

14. WASZCZYSZYN Z., ZIEMIAŃSKI L., 2001, Neural networks in mechanics of structures and materials – new results and prospects of applications, *Computers and Structures*, **79**, 2261-2276

15. WASZCZYSZYN Z., ZIEMIAŃSKI L., 2004, Neural networks in the identification analysis of structural mechanics problems, In: Z. Mroz, G.E. Stavroulakis, eds., *Parameter Identification of Materials and Structures*, CISM Lecture Notes Vol. 469, Springer, Wien-New York (in print)

16. WOLF J.P., SONG C., 1996, *Finite-Element Modelling of Unbounded Media*, John Wiley & Sons, Chichester

17. YAGAWA G., OKUDA H., 1996, Neural networks in computational mechanics, *Archives of Computational Methods in Engineering*, **(3-4)**, 435-512

18. ZIEMIAŃSKI L., 2003, Hybrid neural network/finite element modelling of wave propagation in infinite domains, *Computers and Structures*, **81**, 1099-1109

19. Ziemiański L., Piątkowski G., 2000, Use of neural networks for damage detection in structural elements using wave propagation, In: B.H.V. Topping, editor, *Computational Engineering Using Metaphors from Nature*, 25-30, Edinburgh, Civil-Comp Ltd.

Identyfikacja parametrów konstrukcji na podstawie dynamicznych odpowiedzi z wykorzystaniem sieci neuronowych – wybrane zagadnienia

Streszczenie

W artykule przedstawiono zastosowanie sieci neuronowych w wybranych zagadnieniach dynamiki konstrukcji: 1) wykrywanie uszkodzeń w elementach prętowych na podstawie propagacji fali, 2) dostrajanie modeli MES ram portalowych, 3) wykrywanie pustki i dodatkowej masy w drgającej płycie wspornikowej, 4) modelowanie „sztucznej granicy" w zagadnieniu propagacji fali. Rozpatrywane problemy dotyczą zarówno modeli numerycznych, jak i eksperymentalnych.

Manuscript received February 2, 2004; accepted for print April 26, 2004